Egypt. J. Chem. **Vol. 65**, No. 11 pp. 359 - 373 (2022)

Egyptian Journal of Chemistry

http://ejchem.journals.ekb.eg/

The potential of Chlorella vulgaris (Chlorophyta, Trebouxiophyceae) to reduce carbon dioxide emissions: statistical optimization of carbon dioxide utilization and algal biomass production

Osama A. Swilam*, Ahmed D. El Gamal*, Ehab F. El-Belely*

**Algae Lab, Botany and Microbiology Department, Faculty of Science, Al-Azhar University, Nasr City 11884, Cairo, Egypt.*

Abstract

Global warming is considered one of the most serious and pressing environmental issues in the world, which opens possibilities for finding decisive and effective strategies to reduce the accumulation of gases, especially carbon dioxide emissions. Fortunately, algae mainly depend on CO_2 gas in the photosynthesis process, and the algal biomass produced can be converted into useful and economically valuable materials. The coccoid green microalga *Chlorella vulgaris* is one of the best algal species that can be used as a model in this biotechnology. In the present study, factors affecting the CO_2 consumption, including temperature, pH, light intensity (LI), carbon source availability, and CO_2 supply were statistically optimized using the response surface methodology. The *C. vulgaris* growth was measured by cell count and dry weight, as well as estimating CO_2 content in the culturing medium. The results revealed that the highest algal growth and gas consumption rates were optimized in CO_2-aerated Z-medium and in the presence of a carbon source (Na_2CO_3) at 38 °C, alkaline pH 8.6, and LI 5654 lux. This study sheds the light on the significant potential of microalgae to reduce carbon dioxide emissions as an eco-friendly and renewable strategy for resolving the environmental pollution problems.

Keywords: Algae biomass; Carbon dioxide emissions; *Chlorella vulgaris*; Global warming; Response surface methodology.

1. Introduction

Carbon dioxide (CO_2) is a common greenhouse gas that traps heat from sunlight inside the atmosphere and prevents it from escaping back into space, causing global warming. Carbon dioxide and other heat-trapping gasses, such as methane and nitrous oxide are naturally present in the atmosphere, but the increase in their emissions due to anthropogenic activities has led to the global warming crisis. Each participant in the global economy emits CO_2, but the combustion of fossil fuels and coal-fired power plants followed by diesel generators used in the industrial processes are the main sources of CO_2 emissions. Over the past 10 years, the resulting CO_2 has accounted for about 72% of global greenhouse gases emissions from industrial and human activities [1]. With the exponential growth of population and industrialization, the level of CO_2 in the atmosphere has risen to a point where it is a serious environmental problem. Carbon dioxide is responsible for 60 to 63% of the change in net radiation between different layers of the atmosphere from 1979 to 2004 [2], and thus, global warming could become a critical environmental problem during the 21st century.

Reports of the International Panel on Climate Change (IPCC) have concluded that to limit global warming increases in average global surface temperature to below 2 °C, net human-driven CO_2 emissions must be reduced by the end of this century [3]. Bioenergy with carbon capture and storage (BECCS) is one of the most promising carbon dioxide mitigation strategies involving the growing of plants, including trees and crops, that extract CO_2

*Corresponding author e-mail: Osama_micro@azhar.edu.eg; (O.A. Swilam),
Receive Date: 22 April 2022; Revise Date: 22 May 2022; Accept Date: 08 June 2022.

DOI: 10.21608/ejchem.2022.133254.5948.

from the atmosphere during photosynthesis and storage via carbon injection into geological formations [4].

However, sustainable implementation of most BECCS scenarios on the desired large scale will have extensive environmental consequences, and technical and financial complexities [4-7]. Utilizing biomasses generated from phototrophic microorganisms, such as microalgae and cyanobacteria, is one of the most promising alternatives to reducing CO_2 emissions. Compared to the agricultural production of more conventional crops, the cultivation of photosynthetic microorganisms has much higher expected yields per acre and can be implemented on degraded or unproductive lands [8].

Biological fixation of CO_2 is carried out by both higher plants and photosynthetic microorganisms; however, photosynthetic microorganisms have a greater ability to fix CO_2 compared to higher plants [9-12]. Microalgae and cyanophytes are a large and diverse group of autotrophic microorganisms, which get their energy from photosynthesis, a biological process that involves the bio-fixation of atmospheric carbon dioxide, which can be applied as an attractive approach to offsetting CO_2 emissions through microalgae. However, atmospheric carbon dioxide levels [0.0387% v/v] are not sufficient to support the high microalgal growth rates and productivity needed for large-scale CO_2 elimination, thus, the most efficient way to reduce emissions is the direct bio-fixation of CO_2 from industrial exhaust gases such as flue gas [13]. The flue gas is fully utilized as a resource for microalgae cultivation to mitigate the human impact on our climate and direct the management of microalgae resources towards innovative applications of microalgae biomass compounds. Waste gases from combustion processes typically contain 3-15% (v/v) CO_2; this percentage indicates that the combustion processes will provide sufficient amounts of CO_2 for the production of microalgae on a large scale [14-16].

In the CO_2 bio-fixation strategy, it is important to select microalgal strains with high growth rates, high CO_2-fixing capacity, ability to grow at high CO_2 concentrations and can be easily grown on a large scale to obtain high yields of biomass and active by-products [17]. The genus *Chlorella* (Chlorophyta, Trebouxiophyceae) is a single cell, green eukaryotic microalgae that is quite common to be used in carbon sequestration due to its high photosynthetic efficiency and CO_2-capturing capacity [18]. Moreover, *Chlorella* sp. biomass contains high levels of proteins, carbohydrates, and lipids [19]. *Chlorella vulgaris*, for instance, showed an increase in biomass at a CO_2 concentration of 6% which was 60 times more than at 0.036% of CO_2 concentration, and at both levels, *C. vulgaris* could fix 38.4 and 18.3 mg of CO_2 L day^{-1}, respectively [20]. Sydney [21] reported that with the increase of *C. vulgaris* biomass by 86.68%, the CO_2 fixation rate increased to 251.64 mg L^{-1} day^{-1}. *Chlorella* sp. showed 46% mean CO_2 fixation efficiency, at an input CO_2 concentration of 10% [22], while showing a maximum growth at 10% of CO_2 and lower growth rates from 30 to 50% CO_2 with a wide pH range and temperatures up to 40 °C, while no CO_2 fixation occurred at 70% of CO_2 concentration [23]. *C. vulgaris* showed similar growth rates when allowed to grow at two CO_2 concentrations (2 percent and 13% CO_2 v/v) and three light intensities (50, 120, and 180 $mol.m^{-2}.s^{-1}$) [24]. This study aimed to investigate the effect of different factors on the potential of *C. vulgaris* to achieve the highest growth rate and maximize CO_2 utilization using response surface statistical models.

2. Experimental Section

2.1. Culturing of C. vulgaris

The green microalga *C. vulgaris* was obtained from the Algae Culture Collection at Al-Azhar University (ACCAZ), Cairo, Egypt. The microalgal strain was cultivated in sterilized Z-medium [25] and was illuminated by the cool white fluorescent lamp at 5000 lux under 12/12-h of light/dark cycle and was incubated at 27 ±2 °C. The cultivation medium was made up of macronutrients components (1 ml stock per 1 L media), the stocks included $NaNO_3$ (46.7 g 100 ml^{-1}), Ca $(NO_3)_2.4H_2O$ (5.9 g 100 ml^{-1}), K_2HPO_4 (3.1 g 100 ml^{-1}), $MgSO_4.7H_2O$ (2.5 g 100 ml^{-1}), Na_2CO_3 (2.1 g 100 ml^{-1}), EDTA-$FeCl_3$ solution (10 ml solution per 1 L media) and micronutrients' stock solution (0.08 ml stock per 1L media). *pH* of the medium was set at 6.8 at the onset.

2.2. Growth measurements (cell count and dry weight)

C. vulgaris cells were counted by hemocytometer and the average of cells was calculated from counted small squares and the final cell count (cell ml^{-1}) was calculated using the following equation:

$$\text{Cell count} = \frac{\text{Average cells per small square} \times \text{Dilution factor}}{\text{The volume of a small square (mL)}}$$

Dry weight (DW) was measured by filtering 100 ml of the algal suspension through pre-weighed Whatman filter paper. The filtrate was allowed to dry in the oven at 75 °C to a constant weight. The dry weight (mg ml^{-1}) was calculated as:

DW = [initial weight. (mg) - final weight. (mg)] / 100

2.3. Determination of CO_2 content

The CO_2 content was determined by the titrimetric method [26], using acid titrant, and phenolphthalein at an endpoint of pH 8.3. The CO_2 content was calculated as the following:

$$\text{mg } CO_2\ (L^{-1}) = \frac{A \times N \times 44000}{\text{mL sample}}$$

where: A = mL titrant, and N = normality of NaOH. The CO_2 content was calculated in the case of alkaline titrant using the following equations:

A. Bicarbonate alkalinity

$$HCO_3^{-} \text{ as mg } CaCO_3\ L^{-1} = \frac{T - 5.0 \times 10^{(pH-10)}}{1 + 0.94 \times 10^{(pH-10)}} \quad \ldots \text{ (A)}$$

where, T = total alkalinity, mg $CaCO_3$ L^{-1}.

B. Carbonate alkalinity

$$CO_3^{2-} \text{ as mg } CaCO_3\ L^{-1} = 0.94 \times A \times 10^{(pH-10)} \quad \ldots \text{ (B)}$$

C. Free carbon dioxide

$$\text{mg } CO_2\ L^{-1} = 2.0 \times A \times 10^{(6-pH)} \quad \ldots \text{ (C)}$$

D. Total carbon dioxide

$$\text{mg total } CO_2\ L^{-1} = C + 0.44\ (2A + B)$$

The final growth measurements and CO_2 content were performed after 11 days of the incubation period.

2.4. Statistical optimization using CCD model

The statistical optimization was conducted through response surface methodology (RSM). The most common and highly effective RSM technique used for optimization is the central composite design (CCD). CCD describes the correlation between the factors and response (here were cell count, dry weight, and CO_2 content) using cube points to fit a linear (first-order) model to evaluate the main and interaction effects between factors, the axial points to estimate the quadratic (second-order) polynomial terms, and center points in the cube that contribute to detecting the degree of curvature (quadratic effects) between low and high levels of each factor, and also evaluating the pure experimental error. The mathematical and graphical outputs of the CCD statistical data analysis allow the model to create the optimization curves that predict the final optimal settings of the interacted factors that maximize algal growth (i.e., cell count and DW) and minimize CO_2 content in culture media. All the experimental data of RSM models were generated and analyzed using Minitab® version 18 (2017) extended with statistical and graphical software packages.

A two-level-five-factor (2^5) full factorial CCD was used to evaluate the effect of temperature (z_1), pH (z_2), and light intensity (z_3), at each level of carbon source (with and without), and aeration (air and CD = CO_2). The CCD matrix, including the actual values of the experimental runs at the five levels within each factor, is given in Table 1. Each estimated response variable (Y), obtained from the CCD results, was fitted on a full quadratic (second-order polynomial) multiple regression model as a function of three continuous factors (temperature, pH, and light intensity) at each level of two categorical factors (aeration and carbon source), according to the following equation:

$$Y = \beta_0 + \sum_{i=1}^{k} \beta_i z_i + \sum_{i=1}^{k} \beta_{ii} z_i^2 + \sum_{i=1}^{k-1} \sum_{j=i+1}^{k} \beta_{ij} z_i z_j + \epsilon$$

where, Y is the response; β_0 is the constant intercept coefficient, β_i is the estimated regression coefficients of linear (main effect) terms; β_{ii} is the quadratic coefficient for curvature testing; β_{ij} is the interaction effect coefficients; z_i and z_j are the continuous factors, where $k = 3$ variables, and ϵ is the estimated error terms. Analysis of variance (ANOVA) was utilized to determine the statistical significance of the linear, squared (quadratic), and interaction terms.

2.5. Design and setup of experiments

Eighty Erlenmeyer flasks were filled with 300 ml of *C. vulgaris* culture and divided into 40 flasks with the carbon source (Na_2CO_3), and 40 flasks without the carbon source. Five levels of temperatures (23, 26, 30.5, 35, and 38 °C), five levels of pH (5.3, 6, 7,8, and 8.6), five levels of light intensity (977, 2000, 3500, 5000, and 6023 lux), and two levels of aeration (with natural air or CO_2 at 0.25 L min^{-1} using air bubble stones connected to silicone hoses) were then distributed within each previous group (i.e., with and without carbon source) according to the CCD matrix in Table 1. The flasks were incubated under the appropriate growth conditions with a 12/12 h dark/light cycle.

2.6. The optimization curves

The response optimizer, a tool included in the Minitab® DoE (Design of Experiments) statistical package, was used to generate the optimization curves to determine the final combination settings of the interacted factors that maximize the cell count, dry weight, and minimize the CO_2 content. Individual (d) and composite (D) desirability were used to assess how well (from 0 to 1 scale) the predicted settings maximize the response. This stage was ended by additional confirmation experiments (n = 10

replicated runs) to validate the predicted settings resulting from the optimization curves.

Table (1): Design matrix of 2^5 full factorial CCD and results of *C. vulgaris* cell count×10^4 (cell ml^{-1}), DW (mg ml^{-1}), and CO_2 content (mg L^{-1}) in response to all combinations of low and high levels of interacted factors.

Design points		**Factors**					**Responses**		
Run Order	Point Type	Temp.	pH	LI**	Aeration	C-Source	Cell Count (Cell ml^{-1})*	DW (mg ml^{-1})	CO_2 Cont. (mg L^{-1})
1	1	26	6	2000	Air	With	825	0.585	56.391
2	1	35	6	2000	Air	With	795	0.565	114.870
3	1	26	8	2000	Air	With	730	0.515	216.539
4	1	35	8	2000	Air	With	575	0.630	114.870
5	1	26	6	5000	Air	With	725	0.526	174.136
6	1	35	6	5000	Air	With	560	0.570	114.870
7	1	26	8	5000	Air	With	740	0.545	270.677
8	1	35	8	5000	Air	With	605	0.608	140.914
9	-1	22.9	7	3500	Air	With	721	0.658	207.000
10	-1	38.1	7	3500	Air	With	750	0.585	140.914
11	-1	30.5	5.3	3500	Air	With	725	0.582	114.870
12	-1	30.5	8.7	3500	Air	With	790	0.605	114.870
13	-1	30.5	7	977	Air	With	555	0.510	140.914
14	-1	30.5	7	6022	Air	With	560	0.553	140.914
15	0	30.5	7	3500	Air	With	530	0.528	174.136
16	0	30.5	7	3500	Air	With	600	0.563	114.870
17	0	30.5	7	3500	Air	With	515	0.507	140.914
18	0	30.5	7	3500	Air	With	855	0.641	140.914
19	0	30.5	7	3500	Air	With	650	0.559	140.914
20	0	30.5	7	3500	Air	With	565	0.532	140.914
21	1	26	6	2000	CD	With	1405	0.657	33.216
22	1	35	6	2000	CD	With	1345	0.568	37.204
23	1	26	8	2000	CD	With	1330	0.564	28.843
24	1	35	8	2000	CD	With	1140	0.587	27.416
25	1	26	6	5000	CD	With	1545	0.776	191.400
26	1	35	6	5000	CD	With	1912	0.794	164.600
27	1	26	8	5000	CD	With	1820	0.744	185.000
28	1	35	8	5000	CD	With	2130	0.869	35.426
29	-1	22.9	7	3500	CD	With	1340	0.681	127.101
30	-1	38.1	7	3500	CD	With	1460	0.659	36.450
31	-1	30.5	5.3	3500	CD	With	1575	0.675	87.383
32	-1	30.5	8.7	3500	CD	With	1500	0.670	67.200
33	-1	30.5	7	977	CD	With	830	0.499	19.702
34	-1	30.5	7	6022	CD	With	2177	0.833	178.000
35	0	30.5	7	3500	CD	With	1265	0.618	27.246
36	0	30.5	7	3500	CD	With	1395	0.664	81.770
37	0	30.5	7	3500	CD	With	1425	0.682	71.400
38	0	30.5	7	3500	CD	With	1410	0.678	43.654
39	0	30.5	7	3500	CD	With	1560	0.632	68.461
40	0	30.5	7	3500	CD	With	1475	0.661	33.216
41	1	26	6	2000	Air	Without	885	0.603	114.870
42	1	35	6	2000	Air	Without	675	0.554	216.539
43	1	26	8	2000	Air	Without	805	0.604	216.539
44	1	35	8	2000	Air	Without	720	0.607	140.914
45	1	26	6	5000	Air	Without	700	0.544	188.100
46	1	35	6	5000	Air	Without	600	0.537	140.914
47	1	26	8	5000	Air	Without	920	0.483	270.677
48	1	35	8	5000	Air	Without	550	0.570	174.136
49	-1	22.9	7	3500	Air	Without	830	0.627	270.677

Table (1): Continued.

Design points		Factors					Responses		
Run Order	Point Type	Temp.	pH	LI**	Aeration	C-Source	Cell Count (Cell ml^{-1})*	DW (mg ml^{-1})	CO_2 Cont. (mg L^{-1})
50	-1	38.1	7	3500	Air	Without	700	0.548	140.914
51	-1	30.5	5.3	3500	Air	Without	750	0.566	114.870
52	-1	30.5	8.7	3500	Air	Without	590	0.518	174.136
53	-1	30.5	7	977	Air	Without	775	0.467	140.914
54	-1	30.5	7	6022	Air	Without	590	0.582	140.914
55	0	30.5	7	3500	Air	Without	625	0.540	114.870
56	0	30.5	7	3500	Air	Without	585	0.477	140.914
57	0	30.5	7	3500	Air	Without	690	0.560	140.914
58	0	30.5	7	3500	Air	Without	860	0.536	140.914
59	0	30.5	7	3500	Air	Without	610	0.473	140.914
60	0	30.5	7	3500	Air	Without	720	0.554	140.914
61	1	26	6	2000	CD	Without	1360	0.532	32.306
62	1	35	6	2000	CD	Without	1530	0.535	105.700
63	1	26	8	2000	CD	Without	985	0.492	26.304
64	1	35	8	2000	CD	Without	1175	0.557	26.773
65	1	26	6	5000	CD	Without	1710	0.745	197.700
66	1	35	6	5000	CD	Without	1540	0.716	207.946
67	1	26	8	5000	CD	Without	1825	0.665	205.500
68	1	35	8	5000	CD	Without	1960	0.702	87.500
69	-1	22.9	7	3500	CD	Without	1530	0.736	153.500
70	-1	38.1	7	3500	CD	Without	1455	0.687	127.101
71	-1	30.5	5.3	3500	CD	Without	1525	0.590	50.346
72	-1	30.5	8.7	3500	CD	Without	1365	0.576	30.936
73	-1	30.5	7	977	CD	Without	830	0.515	25.165
74	-1	30.5	7	6022	CD	Without	2000	0.862	196.600
75	0	30.5	7	3500	CD	Without	1455	0.582	93.600
76	0	30.5	7	3500	CD	Without	1660	0.627	100.435
77	0	30.5	7	3500	CD	Without	1510	0.605	39.977
78	0	30.5	7	3500	CD	Without	1705	0.701	56.605
79	0	30.5	7	3500	CD	Without	1495	0.656	35.759
80	0	30.5	7	3500	CD	Without	1615	0.677	68.461

* Cell count $\times 10^4$ cell ml^{-1}. ** LI = Light intensity.

3. Results and discussion

3.1. Cell Count

3.1.1. ANOVA (main and interaction effects)

To determine variations in *C. vulgaris* cell count in response to different factors, a factorial analysis of variance (ANOVA) was performed. The *p*-values and correlation coefficient (r^2) were used to determine the significance ($p \leq 0.05$) of the model and how well the model fits the experimental results. The Main and two-way interaction effects, coefficients of the model, and significance (*p*-value) for the full 2^5 full factorial CCD for cell count are presented in Table (2).

The main effect plots (Fig 1) were created to represent the regression analysis results by representing deviations of the average between the high and low levels within each factor. The results revealed that temperature and pH had no significant difference between low and high levels while the light intensity had a significant effect on the cell count, where the high level of light intensity resulted in a higher mean of the response. The main effect of the aeration shows that pumping CO_2 to the media caused a significant increase in the cell count.

Factors interaction is effective when the change in the response from low to high levels of a factor is dependent on the level of a second factor**;** The interaction effects were also tested by the ANOVA model. For the *C. vulgaris* cell count, the interaction between all two-way terms was significant (Table 2).

The estimated response variable (i.e., cell count), obtained from the ANOVA model, was subsequently

fitted to a full quadratic (second-order polynomial) multiple regression model, but due to there were no significant quadratic (square) terms the equation was simplified by eliminating the square terms as follow:

$$\text{Cell count}_{Air} = 2540 - 11.55\,\text{Temp.} - 202.9\,\text{pH} - 0.4041\,\text{LI} + 0.0545\,\text{pH} \times \text{LI}$$

$$\text{Cell count}_{CD} = 2004 + 6.73\,\text{Temp.} - 202.9\,\text{pH} - 0.1766\,\text{LI} + 0.0545\,\text{pH} \times \text{LI}$$

3.1.2. The Pareto charts and normal probability plots

The relative importance and the significance of the main and interactions effects were determined by the Pareto chart (Figure, 2 A).

Table (2): Results of ANOVA model to test for differences in *C. vulgaris* cell count in response to different factors. Significant differences are denoted in bold. (r^2 = 94.83%).

Source	*df*	Adj SS	Adj MS	*F*-Value	Coef	*P*-Value
Model	7	16318760	2331251	172.74		**0.000**
Linear (Main Effect)	4	14422768	3605692	267.17		**0.000**
Temp.	1	6419	6419	0.48	-10.8	0.493
pH	1	7901	7901	0.59	-12.0	0.447
LI	1	1027603	1027603	76.14	137.2	**0.000**
Aeration	1	13380844	13380844	991.48	-409.0_{Air}	**0.000**
2-Way Interaction	3	1895992	631997	46.83		**0.000**
Temp. × Aeration	1	92471	92471	6.85	-41.1	**0.011**
pH × LI	1	214185	214185	15.87	81.8	**0.000**
LI × Aeration	1	1589336	1589336	117.77	-170.6_{Air}	**0.000**
Error	72	971699	13496			
Lack-of-Fit	52	743878	14305	1.26		0.294
Pure Error	20	227821	11391			
Total	79	17290459				

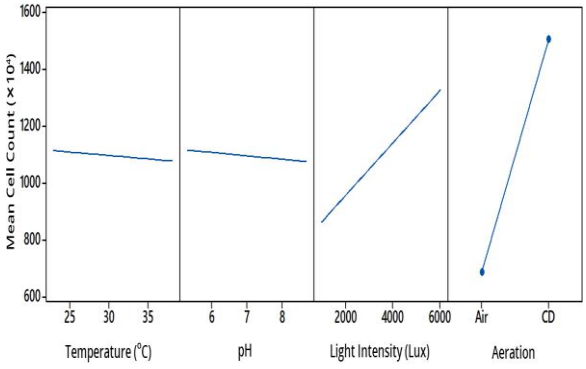

Fig. (1): Main effects plots explain the changes in *C. vulgaris* cell count (cell ml^{-1}) between low and high levels of each factor.

A student's *t*-test was conducted to determine whether the calculated effects were significantly different from zero, these values for each effect are shown in the Pareto chart by horizontal columns. The *t*-value was1.99 for the count, these values exceed a reference line, corresponding to the 95% confidence interval, and are considered to have a significant effect on the cell count.

Pareto chart of the standardized effects for cell count (Figure 2 A) revealed that the main effect of aeration (D), the interaction between light intensity and aeration (CD), light intensity (C), the interaction between pH and light intensity (BC) and interaction between temperature and aeration (AD) are extended beyond the reference line and indicating a significant effect of these terms at level of $p \leq 0.05$, while the relative importance of each term is represented by the column length.

The normal probability plot determines the actual (real) effect of each term; therefore, it is indicating if the results occurred by chance (random) or not.

Moreover, normal probability plots determine whether the term causes a negative or positive effect on the response, where the positive effect means an increase in the factor causes an increase in the response and vice versa for a negative effect. Each effect is given a single point on the plot and the points that are close to a fitted line (refers to the position where the effects were zero) represent the estimated factors that have no significant effect on the response, while the actual (real) term effect is represented by points far away from the fitted line.

The main terms of light intensity (C) followed by interaction between pH and light intensity (BC) are far away from the fitted straight line, indicating a strong significant impact on the cell count, furthermore, their contribution had a positive effect due to it is located at the right side of the graph (Figure 2 B). On the other hand, the aeration (D), the interaction between light intensity and aeration (CD), and the interaction between temperature and aeration (AD) are located at the left of the fitted line, indicating a significant negative effect on the cell count (Figure 2 B).

3.1.3. Contour and surface plots

Based on the significance of main and two-way interaction effects, the contour and surface plots were established to visually fit the increasing cell count of each two-factor and hold the third factor that is not included in the plot constant. The contour plot is a two-dimensional graph in which all points, one point from each plotted factor, that have the same response value are connected to form a zonation (i.e., contour lines) from minimum to maximum response (count) values.

A surface-wireframe plot is a three-dimensional graph that displays the relationship between the response and each two interacted process factors. The relation is represented by a 3D grid (wireframe) plot that shows the optimum peaks of the highest response values. The surface plots of the response functions

are useful in a clearer understanding of main, square, and interaction effects.

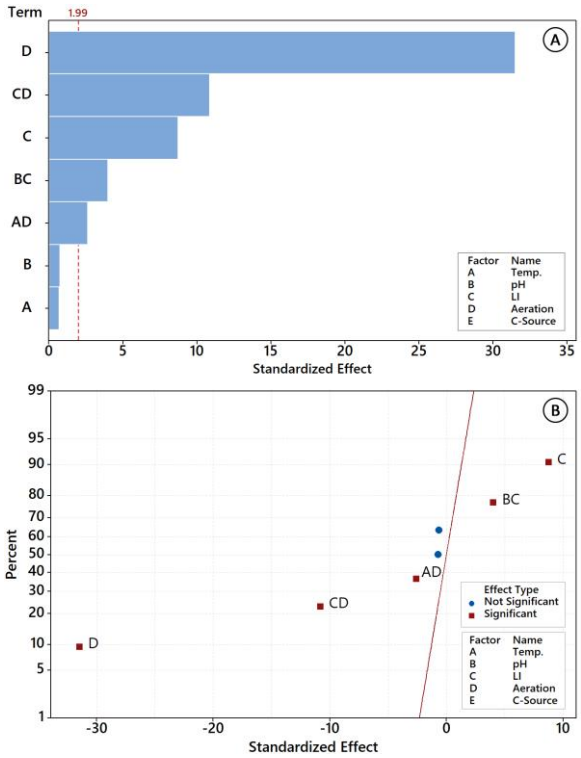

Fig. (2): Pareto chart (A) and normal probability plot (B) of standardized effects on. *C. vulgaris* cell count (cell ml^{-1}).

A typical simple maximum pattern occurred in the contour and surface plots of the cell count between temperature and pH at exposure to air (Figure 3 A and B), where the cell count increased up to 760×10^4 cell ml^{-1} at a lower temperature (25 °C) and wide pH range from 5 to 8. In case of exposure to CO_2 (Figure 3 C and D), the cell count increased to 1600×10^4 cell ml^{-1} at 37.5 °C and acidic pH of ~ 5. On the other hand, at pH ~ 5.5 and a light intensity of ~ 1500 lux, the cell count was higher (around 900×10^4 cell ml^{-1}) when the medium was aerated with natural air (Figure 4 A and B), while with CO_2 the count increased to about 2200×10^4 cell ml^{-1} at high light intensity (6000 lux) and pH of 9.

Figure 4 A and B showed that the cell count reaches 850×10^4 cell ml^{-1} when the culture was aerated by air at low temperature (25 °C) and low light intensity (~ 2000 lux) while in media supplemented with CO_2, the count was about 2200×10^4 cell ml^{-1} at a higher temperature of 37.5 °C and light intensity at 6000 lux (Figure 4 C and D).

The interaction between LI and temperature revealed that an increase in the cell count (up to 800×10^4 cell ml^{-1}) occurred at low temperature (less than 25 °C) and low light intensity (1000 to 2000 lux) when the media supplemented with air (Figure 5 A and B), however a higher cell count (about 2000×10^4 cell ml^{-1}) was determined at a high light intensity of 6000 lux and temperature ranged from 22.5 to 30°C with CO_2 aeration (Figure 5 C and D).

Photosynthesis in microalgal, and subsequent carbon dioxide fixation process are all depending on light intensity [27, 28].

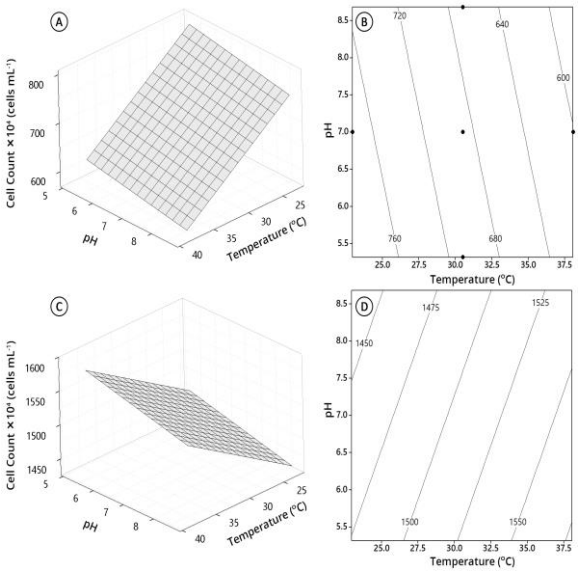

Fig. (3): Surface (A and C) and contour (B and D) plots of the effect of temperature (°C) and pH on *C. vulgaris* cell count at aeration with air (A and B) and CO_2 (C and D), at a constant value of LI = 3500 lux.

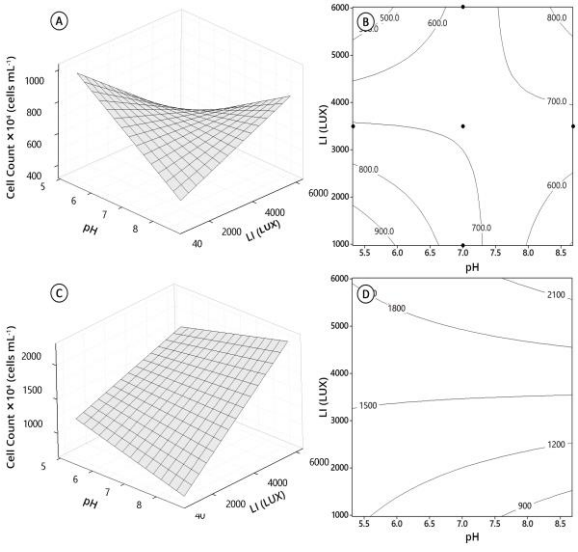

Fig. (4): Surface (A and C) and contour (B and D) plots of the effect of LI (lux) and pH on *C. vulgaris* cell count at aeration with air (A and B) and CO_2 (C and D), at a constant value of temperature = 35.5 °C.

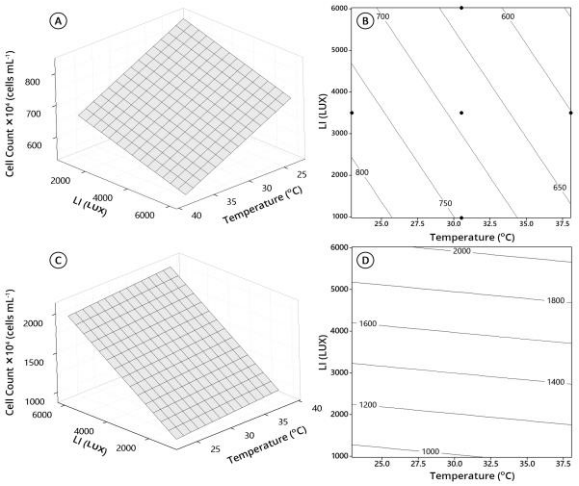

Fig. (5): Surface (A and C) and contour (B and D) plots of the effect of LI (lux) and temperature (°C) on *C. vulgaris* cell count at aeration with air (A and B) and CO_2 (C and D), at a constant value of pH = 7.

Our results have revealed that the higher light intensities, around 6000 lux, made the media saturated with photons that were sufficient to cause a rapid photosynthesis rate which cause more cell divisions when the media was aerated by CO_2, that used as a carbon source, causing increasing of cell count compared to aeration by natural air. The efficiency of the photosynthetic process was related to high temperatures (around 37.5 °C) associated with high light intensity causing optimal cell division and therefore cell count maximization, this agrees with Ras et al., 2013 [29] who investigated the impacts of temperature on numerous microalgae species, focusing on metabolic consequences and adaptation to high temperature.

Because pH impacts the activity of several enzymes, it is also one of the most critical parameters for algal growth [30]**.** Many researchers [31-35] concluded that the ideal pH for growth is generally in the neutral to the slightly alkaline range of 6–8.3, and this agrees with our experiments, where cell count reached the maximum value at pH of about 9. In general, cell division depended significantly on the interaction between temperature, light intensity, and pH.

3.2. Dry weight (DW)

3.2.1. ANOVA (main and interaction effects)

ANOVA was used to detect the differences in *C. vulgaris* dry weight in response to different conditions. Table (3) displays the main and two-way interaction effects, model coefficients, and significance (*p*-value) for the full 2^5 full factorial CCD.

The results (Table 3 and Figure 6) revealed that the temperature and pH have no significant difference in the dry weight between low and high levels, however, a significant curvature effect of temperature (Temp. × Temp.) was detected between the low and high levels. Pumping of CO_2 to the media, high light intensity and presence of carbon sources have significant effects on the dry weight. The two-way interaction between temperature and pH; and between LI and aeration was significantly affecting the DW.

Table (3): Results of ANOVA model to test for differences in *C. vulgaris* DW (mg ml^{-1}) in response to different factors. Significant differences are denoted in bold. (r^2 = 81.63%).

Source	*df*	Adj SS	Adj MS	*F*-Value	Coef	*P*-Value
Model	8	0.503625	0.062953	39.44		**0.000**
Linear (Main Effect)	5	0.341252	0.068250	42.75		**0.000**
Temp.	1	0.000004	0.000004	0.00	0.00026	0.962
pH	1	0.000354	0.000354	0.22	-0.00254	0.639
LI	1	0.128555	0.128555	80.53	0.04851	**0.000**
Aeration	1	0.195229	0.195229	122.30	-0.0494_{Air}	**0.000**
C-Source	1	0.017111	0.017111	10.72	0.0146_{With}	**0.002**
Square Effect	1	0.017951	0.017951	11.24		**0.001**
Temp.×Temp.	1	0.017951	0.017951	11.24	0.01749	**0.001**
2-Way Interaction	2	0.144422	0.072211	45.24		**0.000**
Temp.×pH	1	0.013082	0.013082	8.19	0.02022	**0.006**
LI×Aeration	1	0.131340	0.131340	82.28	-0.049_{Air}	**0.000**
Error	71	0.113341	0.001596			
Lack-of-Fit	51	0.081537	0.001599	1.01		0.516
Pure Error	20	0.031803	0.001590			
Total	79	0.616966				

A full quadratic (second-order polynomial) multiple regression model was fitted as the following:

Aeration	C-Source			
Air	With	DW	=	2.341 - 0.0841 Temp. - 0.1396 pH - 0.000000 LI + 0.000864 Temp.×Temp. + 0.00449 Temp.×pH
CD	With	DW	=	2.210 - 0.0841 Temp. - 0.1396 pH + 0.000065 LI + 0.000864 Temp.×Temp. + 0.00449 Temp. ×pH
Air	Without	DW	=	2.311 - 0.0841 Temp. - 0.1396 pH - 0.000000 LI + 0.000864 Temp.×Temp. + 0.00449 Temp.×pH
CD	Without	DW	=	2.181 - 0.0841 Temp. - 0.1396 pH + 0.000065 LI + 0.000864 Temp.×Temp. + 0.00449 Temp.×pH

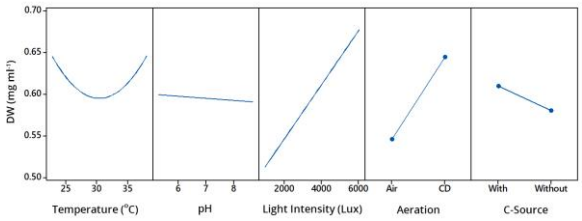

Fig. (6): Main effects plots explain the changes in *C. vulgaris* DW (mg ml^{-1}) between low and high levels of each factor.

3.2.2. The Pareto charts and normal probability plots

Pareto chart of the standardized effects for DW (Figure 7 A) showed that the main effect of aeration (D), the interaction between light intensity and aeration (CD), light intensity (C), the square effect of temperature (AA), presence of carbon source (E) and the interaction between temperature and pH (AB) are expanded beyond the reference line, indicating that these terms have a significant influence as well as respective relative importance on *C. vulgaris* biomass.

The main terms of aeration (D) followed by interaction between light intensity and aeration (CD) indicate a strong significant negative impact on the DW, while the other significant terms show a positive effect, as shown in Figure 7 B.

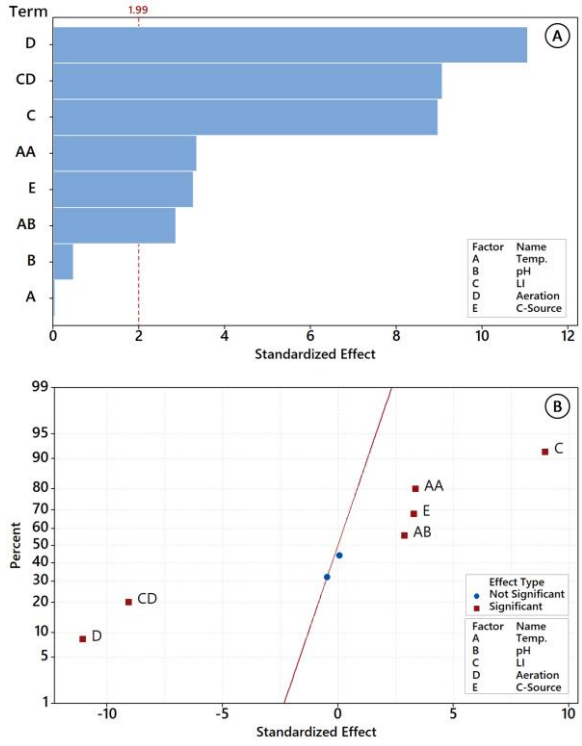

Fig. (7): Pareto chart (A) and normal probability plot (B) of standardized effects on *C. vulgaris* DW (mg ml^{-1}).

3.2.3. Contour and surface plots

The *C. vulgaris* dry weight was significantly affected by the interaction between temperature and pH at exposure to air in the presence or absence of a carbon source (Figure 8). The results indicated that DW increased to about 0.7 mg ml^{-1} at low temperature (~20 °C) and acidic pH (~5), and in the opposite levels, increased to similar values at high temperature (~37.5 °C) and alkaline pH (~8.5) causing a negative curvature effect of temperature lead to DW deficiency at the center points.

The interaction between temperature and light intensity showed a DW of 0.6 mg ml^{-1} in both media with and without carbon source and aerated with normal air (Figure 9 A and B) at a wide range of light intensity (1000-6000 lux) with a typical curvature effect between low and high temperature (20 and 37.5 °C, respectively).

Figure 10 also revealed that dry weight had the highest values at a wide range of light intensity (1000 to 6000 lux) at a pH of about 5.5 when media aerated by air and carbon source is present.

Biomass production in microalgae species rises with increasing light intensity, due to increased absorption and utilization of the light by the photosynthetic system. Photo-inhibition may occur at high to extreme light intensities, beyond the saturation point, causing photo-oxidation within the algal cells [36]. Our results indicated that *C. vulgaris* gave high levels of biomass production at a wide range of light intensities especially when media supplemented with CO_2.

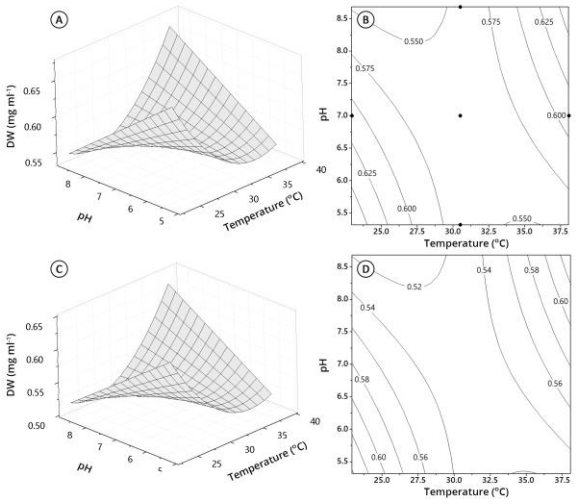

Fig. (8): Surface (A and C) and contour (B and D) plots of the effect of pH and temperature (°C) on *C. vulgaris* DW at aeration with air with a normal carbon source (A and B) and without carbon source (C and D), at a constant value of LI = 3500 lux.

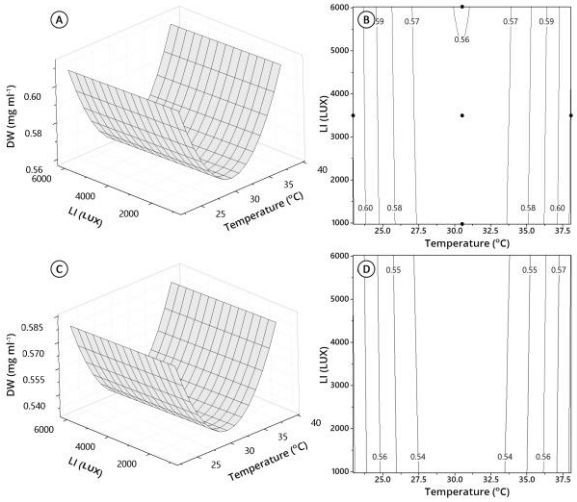

Fig. (9): Surface (A and C) and contour (B and D) plots of the effect of LI (lux) and temperature (°C) on *C. vulgaris* DW at aeration with air with a normal carbon source (A and B) and without carbon source (C and D), at a constant value of pH = 7.

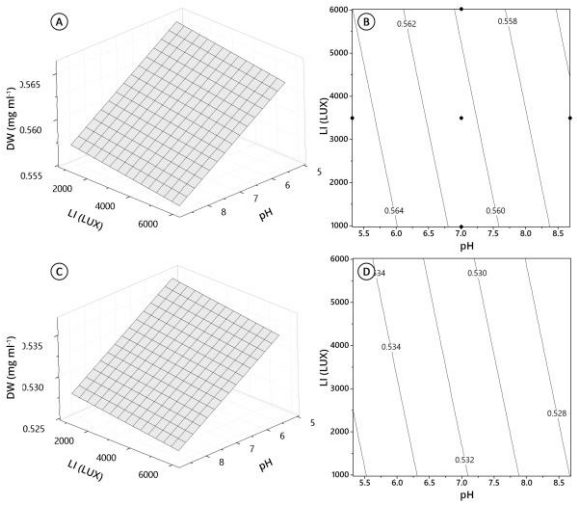

Fig. (10): Surface (A and C) and contour (B and D) of the effect of LI (lux) and pH on *C. vulgaris* DW at aeration with Air with a normal carbon source (A and B) and without carbon source (C and D), at a constant value of temperature = 35.5 °C.

Several studies have shown that *C. vulgaris* can grow at high rates when exposed to high light intensity [36-38]. *pH* is also a critical factor for microalgae cultivation, it is a key environmental element that influences cell development and biomass creation [39]. *Chlorella* sp. can grow in a wide pH range (4-10), with alkaline circumstances of pH 9 to 10, yielding the highest biomass output [40]. In this study, *C. vulgaris* biomass also increased in the direction of acidic and alkaline pH (i.e., 5 and 8.5, respectively).

Temperature is one of the important factors that control the metabolism and biological processes inside the algal cell [41]. In agreement with the results we obtained, it was found that *C. vulgaris* gives high biomass productivities at temperatures ranging from 20 to 36 °C [42], especially when aerated by CO_2 flow compared with aeration by natural air [41].

3.3. Total CO_2 Content

The CO_2 content measurement was intended to be the rate of gas consumption in the cultivation medium, so a lower content indicates a greater carbon dioxide consumption.

3.3.1. ANOVA (main and interaction effects)

The results in table 4 and Figure 11 demonstrated that pH had no significant effect on total CO_2 content at low and high levels, but there were significant main effects between low and high levels for temperature, light intensity, aeration, and carbon source.

Significant curvature effects were detected in the square term for the temperature and light intensity, where the lowest CO_2 content was detected at the center point of temperature (i.e., at 30 °C) and low light intensity at 2000 lux. The two-way interaction terms indicated that the effect of both temperature and aeration was depending on the levels of pH and light intensity. In general, the minimization of the total CO_2 content occurred when media are aerated with CO_2 and in the presence of the carbon source (Table 4 and Figure 11).

Table (4): Results of ANOVA model to test for differences in total CO_2 content (mg L^{-1}) in response to different factors. Significant differences are denoted in bold. (r^2 = 86.24%).

Model	11	286509	26046.3	38.75		**0.000**
Linear (Main Effect)	5	182056	36411.2	54.17		**0.000**
Temp.	1	21504	21504.0	31.99	-19.84	**0.000**
pH	1	223	222.9	0.33	2.02	0.567
LI	1	58965	58965.3	87.73	32.85	**0.000**
Aeration	1	95708	95707.8	142.39	34.59_{Air}	**0.000**
C-Source	1	5656	5656.1	8.42	-8.41_{With}	**0.005**
Square Effect	2	27068	13534.1	20.14		**0.000**
Temp.×Temp.	1	22993	22993.4	34.21	19.87	**0.000**
LI×LI	1	5971	5970.6	8.88	10.13	**0.004**
2-Way Interaction	4	77385	19346.2	28.78		**0.000**
Temp.×pH	1	19338	19338.2	28.77	-24.58	**0.000**
Temp.×LI	1	14287	14287.4	21.26	-21.13	**0.000**
pH×Aeration	1	16111	16111.4	23.97	17.17_{Air}	**0.000**
LI×Aeration	1	27648	27648.0	41.13	-22.50_{Air}	**0.000**
Error	68	45705	672.1			
Lack-of-Fit	48	37196	774.9	1.82		0.072
Pure Error	20	8509	425.5			
Total	79	332214				

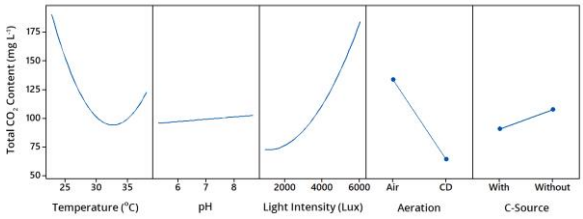

Fig. (11): Main effects plots explain the changes in total CO_2 content in relation to low and high levels of each factor.

A full quadratic (second-order polynomial) multiple regression model was fitted in uncoded units of aeration and carbon source as the following:

Aeration	C-Source			
Air	With	Total CO_2	=	-431 - 15.1 Temp. + 185.8 pH + 0.0709 LI + 0.981 Temp.×Temp. + 0.000005 LI×LI - 5.46 Temp.×pH - 0.003130 Temp.×LI
CD	With	Total CO_2	=	-365 - 15.1 Temp. + 151.5 pH + 0.1009 LI + 0.981 Temp.×Temp. + 0.000005 LI×LI - 5.46 Temp.×pH - 0.003130 Temp.×LI
Air	Without	Total CO_2	=	-414 - 15.1 Temp. + 185.8 pH + 0.0709 LI + 0.981 Temp.×Temp. + 0.000005 LI×LI - 5.46 Temp.×pH - 0.003130 Temp.×LI
CD	Without	Total CO_2	=	-348 - 15.1 Temp. + 151.5 pH + 0.1009 LI + 0.981 Temp.×Temp. + 0.000005 LI×LI - 5.46 Temp.×pH - 0.003130 Temp.×LI

3.3.2. The Pareto charts and normal probability plots

The Pareto chart for the total CO_2 content (Figure 12 A) showed that the main effects of aeration (D), and light intensity (C); the LI and aeration interaction (CD), the square effect of temperature (AA), the main effect of temperature (A), the temperature and pH interaction (AB), the pH and aeration interaction (BD), the temperature and LI interaction (AC), the square effect of LI (CC) and the main effect of carbon source (E) were beyond the reference line, which means that these terms have a significant influence and respective relative importance on CO_2 content.

The square effect of LI (CC), followed by the interaction between pH and aeration (BD), the square effect of temperature (AA), LI (C), and aeration (D) are all far from the fitted straight line and located at the right side of the normal probability plot (Figure 12 B), implying that each term had a significant positive impact on total CO_2 content, while the other significant terms had a negative impact on the CO_2 content.

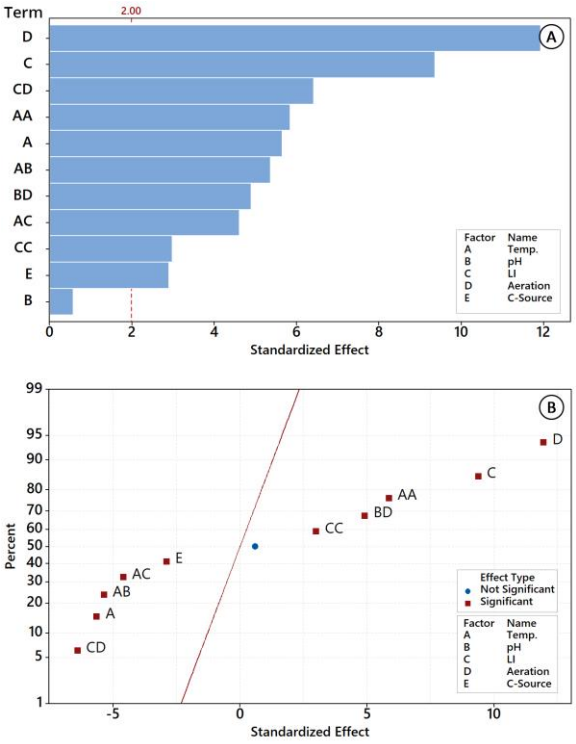

Fig. (12): Pareto chart (A) and normal probability plot (B) of standardized effects on total CO_2 content (mg L^{-1}).

3.3.3. Contour and surface plots

The contour and surface plots of the total CO_2 content that explain the interactions between temperature and pH at exposure to air and CO_2 are shown in Figures 13 and 14, respectively. When the culturing media was supplemented with air, a typical reduction of the total carbon dioxide content to 100 mg L^{-1} occurred in the temperature range from 25 to 31 °C and acidic pH (~5.5) in the presence of the carbon source (Figure 13 A and B), while in the absence of carbon source (Figure 13 C and D), the CO_2 content minimized to 150 mg L^{-1} at a wide range of temperature (20-35 °C) and pH (5.5- 8.5). *C. vulgaris* consumed all CO_2 content when media was aerated by CO_2 in presence of carbon source at a high temperature of around 36 °C and alkaline of pH at 8.5 (Figure 14 A and B) while in the absence of carbon source at the same condition the total CO_2 content minimized to 50 mg L^{-1} (Figure 14 C and D).

The interaction between light intensity (LI) and temperature showed that a minimum CO_2 content of 150 mg L^{-1} was recorded over a wide range of LI (1000-6000 lux) and temperature (25-37 °C) when air is supplied to culturing medium with no considerable difference between the presence or absence of carbon source, as shown in Figure 15 A-D. However, CO_2 content dropped to a value of zero at a pointed light

intensity of 1000 lux and a range of temperature from 25 to 32.5 °C when the media was aerated with CO_2 and supplemented with the normal carbon source (Figure 16 A and B), while the minimum CO_2 content was 50 mg L^{-1} when the media did not contain a carbon source (Figure 16 C and D).

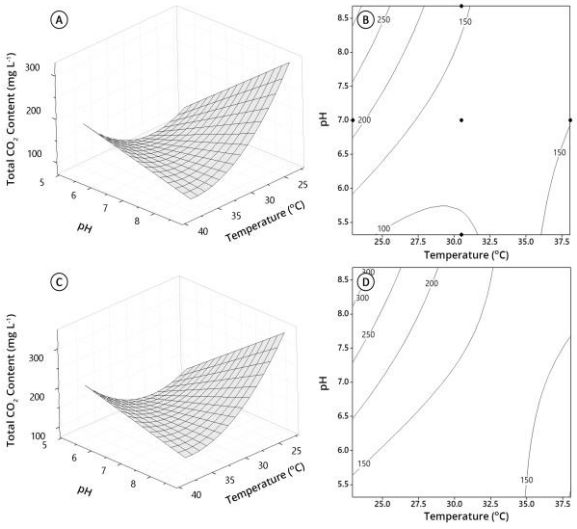

Fig. (13): Surface (left) and contour (right) plots of the effect of pH and temperature (°C) on total CO_2 content at aeration with air with a normal carbon source (A and B) and without carbon source (C and D), at a constant value of LI = 3500 lux.

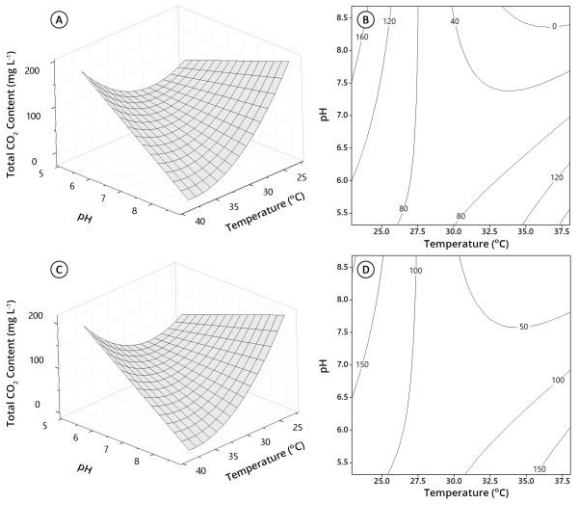

Fig. (14): Surface (left) and contour (right) plots of the effect of pH and temperature (°C) on total CO_2 content at aeration with CO_2 with a normal carbon source (A and B) and without carbon source (C and D), at a constant value of LI = 3500 lux.

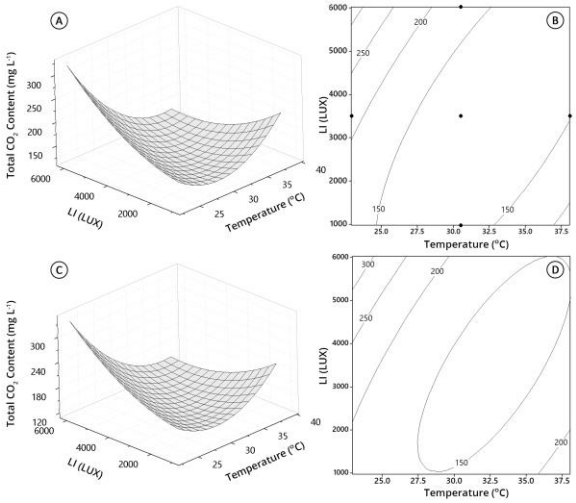

Fig. (15): Surface (left) and contour (right) plots of the effect of LI and temperature (°C) on total CO_2 content at aeration with air with a normal carbon source (A and B) and without carbon source (C and D), at a constant value of pH = 7.

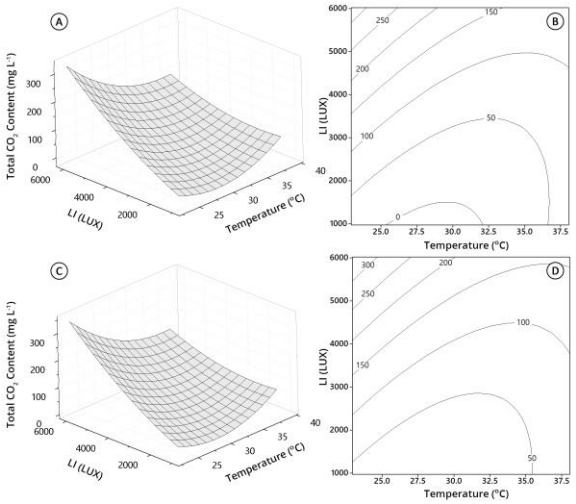

Fig. (16): Surface (left) and contour (right) plots of the effect of LI and temperature (°C) on total CO_2 content at aeration with CO_2 with a normal carbon source (A and B) and without carbon source (C and D), at a constant value of pH = 7.

In algae, photosynthesis is the process that is determined by many environmental factors (such as temperature and pH) and involves light absorption and CO_2 bio-fixation [27, 28]. The ability of algae to utilize CO_2 is controlled by physiological conditions (i.e., strain-dependent) and CO_2-solubility which is a temperature-dependent phenomenon [43, 44]. When the carbon dioxide dissolved in the aqueous culturing media it can be exist as carbon dioxide, HCO^{3-}, CO_3^{2-} and H_2CO_3. Carbon dioxide and HCO^{3-} are the two most common species utilized by microalgal cells [45].

3.4. The optimization curves

The response optimizer tool was used to generate the optimization curves (Figure 17) to determine the final optimal settings of the factors that maximize cell count and DW of *C. vulgaris* and minimize the CO_2 content. Based on the predicted settings obtained from the optimization curves, and to achieve the optimal goals, including maximizing the cell number to 2177×10^4 cell ml^{-1} (individual desirability = 100%), maximizing the DW to 0.9 mg ml^{-1} (individual desirability = 100%), and reducing the CO_2 content to 33.6 mg L^{-1} (individual desirability = 98.12%), ten replicated confirmatory runs were prepared and incubated according to the proposed conditions, which were a temperature of 38.1 °C, pH at 8.7, LI at 5654 lux, and the cultures were aerated with carbon dioxide, and supplemented with the carbon sources. Results of the confirmatory runs were plotted to compare the actual values (mean ±standard deviation) with the values predicted by the model (Figure 18). The results revealed that the mean of actual cell count was 2213×10^4 ($\pm183.31\times10^4$) cell ml^{-1}, DW was 0.97 (±0.15) mg ml^{-1}, and CO_2 content was 19.73 (±13.78) mg L^{-1}.

4. Conclusion

In this study, at the conclusion of the experiments, cell count, DW, and the carbon dioxide levels in the culturing medium were used to measure the potential of *C. vulgaris* in reducing the carbon dioxide emissions and producing useful and economically valuable biomass. It was concluded that the algae consumed from 92.7 to 100% of the carbon dioxide content and produce 0.97 mg $ml^{-1}$of dried biomass, with a total cell count of 2213×10^4 cell ml^{-1}, this, in turn, demonstrates the ability of *C. vulgaris* to organically reduce CO_2 emissions, which should be pursued in the future.

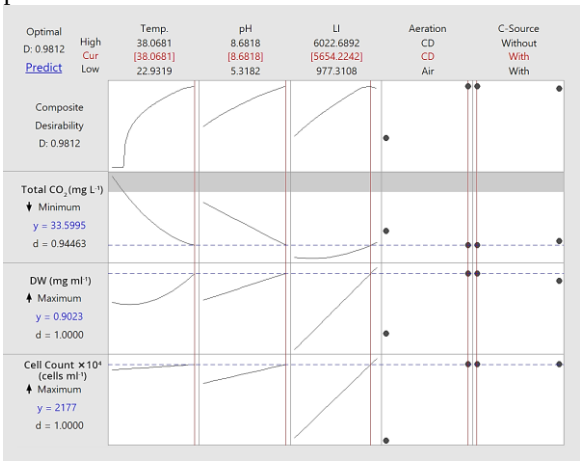

Fig. (17): The optimization curves show how the factors affect the predicted responses (y) including minimum total CO_2 content; and maximum DW and cell count, at low and high levels. The optimum factor settings (Cur) were predicted with a composite desirability (D) = 0.9812 (98.12%).

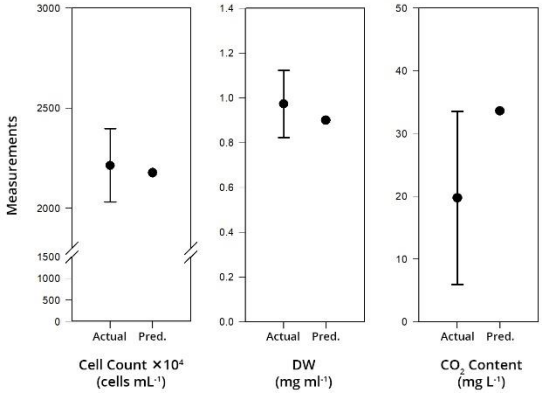

Fig. (18): Scatter plot, comparing the actual (n = 10) and predicted (Pred.) values of cell count, DW, and CO_2 content. Error bars represent standard deviations.

Conflicts of interest

There are no conflicts to declare.

5. References

[1] J.G.J. Olivier, J.A.H.W. Peters, Trends in global CO_2 and total greenhouse gas emissions: 2020 report., in, PBL Netherlands Environmental Assessment Agency, The Hague, 2020, pp. 1-85.

[2] D.J. Hofmann, J.H. Butler, E.J. Dlugokencky, J.W. Elkins, K. Masarie, S.A. Montzka, P. Tans, The role of carbon dioxide in climate forcing from 1979 to 2004: introduction of the Annual Greenhouse Gas Index, Tellus B: Chemical and Physical Meteorology, 58 (2006) 614–619.

[3] M.R. Allen, O.P. Dube, W. Solecki, F. Aragón-Durand, W. Cramer, S. Humphreys, M. Kainuma, J. Kala, N. Mahowald, Y. Mulugetta, R. Perez, M. Wairiu, K. Zickfeld, Framing and Context, in: V. Masson-Delmotte, P. Zhai, H.-O. Pörtner, D. Roberts, J. Skea, P.R. Shukla, A. Pirani, W. Moufouma-Okia, C. Péan, R. Pidcock, S. Connors, J.B.R. Matthews, Y. Chen, X. Zhou, M.I. Gomis, E. Lonnoy, T. Maycock, M. Tignor, T. Waterfield (Eds.) Global Warming of 1.5°C. An IPCC Special Report on the impacts of global warming of 1.5°C above pre-industrial levels and related global greenhouse gas emission pathways, in the context of strengthening the global response to the threat of climate change, sustainable development, and efforts to eradicate poverty, Intergovernmental Panel on Climate Change, 2018, pp. 49-91.

[4] C. Gough, P. Upham, Biomass energy with carbon capture and storage (BECCS or Bio-CCS), Greenhouse Gases: Science and Technology, 1 (2011) 324-334.

[5] N.R. Council, Climate Intervention: Carbon Dioxide Removal and Reliable Sequestration, The National Academies Press, Washington, DC, 2015.

[6] K. Anderson, G. Peters, The trouble with negative emissions, Science, 354 (2016) 182-183.

[7] C. Gough, S. Garcia-Freites, C. Jones, S. Mander, B. Moore, C. Pereira, M. Röder, N. Vaughan, A. Welfle, Challenges to the use of BECCS as a keystone technology in pursuit of 1.5 ºC, J Global Sustainability, 1 (2018).
[8] A.F. Clarens, E.P. Resurreccion, M.A. White, L.M. Colosi, Environmental life cycle comparison of algae to other bioenergy feedstocks, Environmental Science & Technology, 44 (2010) 1813-1819.
[9] Y. Chisti, Biodiesel from microalgae, Biotechnology advances, 25 (2007) 294-306.
[10] Y. Li, M. Horsman, N. Wu, C.Q. Lan, N. Dubois-Calero, Biofuels from microalgae, Biotechnology Progress, 24 (2008) 815-820.
[11] M.R. Tredici, Photobiology of microalgae mass cultures: understanding the tools for the next green revolution, Biofuels, 1 (2010) 143-162.
[12] M.K. Lam, K.T. Lee, A.R. Mohamed, Current status and challenges on microalgae-based carbon capture, International Journal of Greenhouse Gas Control, 10 (2012) 456-469.
[13] C.-Y. Kao, T.-Y. Chen, Y.-B. Chang, T.-W. Chiu, H.-Y. Lin, C.-D. Chen, J.-S. Chang, C.-S. Lin, Utilization of carbon dioxide in industrial flue gases for the cultivation of microalga *Chlorella* sp., Bioresource Technology, 166 (2014) 485-493.
[14] M. Packer, Algal capture of carbon dioxide; biomass generation as a tool for greenhouse gas mitigation with reference to New Zealand energy strategy and policy, Energy Policy, 37 (2009) 3428-3437.
[15] Y. Jiang, W. Zhang, J. Wang, Y. Chen, S. Shen, T. Liu, Utilization of simulated flue gas for cultivation of *Scenedesmus dimorphus*, Bioresource Technology, 128 (2013) 359-364.
[16] M.A. Vale, A. Ferreira, J.C.M. Pires, A.L. Gonçalves, Chapter 17 - CO_2 capture using microalgae, in: M.R. Rahimpour, M. Farsi, M.A. Makarem (Eds.) Advances in Carbon Capture, Woodhead Publishing, 2020, pp. 381-405.
[17] A. Aslam, T.A. Mughal, A review on microalgae to achieve maximal carbon dioxide (CO_2) mitigation from industrial flue gases, International Journal of Research in Advent Technology, 4 (2016) 12-29.
[18] M.K. Lam, K.T. Lee, Effect of carbon source towards the growth of *Chlorella vulgaris* for CO_2 bio-mitigation and biodiesel production, International Journal of Greenhouse Gas Control, 14 (2013) 169-176.
[19] J. Verspreet, L. Soetemans, C. Gargan, M. Hayes, L. Bastiaens, Nutritional Profiling and preliminary bioactivity screening of five micro-algae strains cultivated in Northwest Europe, Foods, 10 (2021) 1516.
[20] S. Chinnasamy, B. Ramakrishnan, A. Bhatnagar, K.C. Das, Biomass production potential of a wastewater alga *Chlorella vulgaris* ARC 1 under elevated levels of CO_2 and temperature, International journal of molecular sciences, 10 (2009) 518-532.
[21] E.B. Sydney, Respirometric Balance and Analysis of four microalgae: Dunaliella tertiolecta, *Chlorella vulgaris*, *Spirulina platensis* and *Botryococcus braunii*, in, Dissertação (Mestrado em Processos Biotecnológicos) Universidade Federal do …, 2009.
[22] R. Ramanan, K. Kannan, A. Deshkar, R. Yadav, T. Chakrabarti, Enhanced algal $CO_{(2)}$ sequestration through calcite deposition by *Chlorella* sp. and *Spirulina platensis* in a mini-raceway pond, Bioresource technology, 101 (2010) 2616-2622.
[23] K.D. Sung, J. Lee, C. Shin, S. Park, Isolation of a new highly CO_2 tolerant fresh water microalga *Chlorella* sp. KR-1, Renewable energy, 16 (1999) 1019-1022.
[24] B. Clément-Larosière, F. Lopes, A. Gonçalves, B. Taidi, M. Benedetti, M. Minier, D. Pareau, Carbon dioxide biofixation by *Chlorella vulgaris* at different CO_2 concentrations and light intensities, Engineering in Life Sciences, 14 (2014) 509-519.
[25] R. Staub, Ernährungsphysiologisch-autökologische Untersuchungen an der planktischen Blaualge*Oscillatoria rubescens* DC, Schweizerische Zeitschrift für Hydrologie, 23 (1961) 82-198.
[26] D.A. Vaccari, Standard methods for the examination of water and wastewater, Choice: Current Reviews for Academic Libraries, 49 (2012) 1-2316.
[27] T. Costache, F.G. Acien Fernandez, M. Morales, J. Fernández-Sevilla, I. Stamatin, Molina, Comprehensive model of microalgae photosynthesis rate as a function of culture conditions in photobioreactors, Applied microbiology and biotechnology, 97 (2013) 7627-7637.
[28] I. Fernández, F. Acién, J. Fernández, J. Guzmán, J. Magán, M. Berenguel, Dynamic model of microalgal production in tubular photobioreactors, Bioresource technology, 126 (2012) 172-181.
[29] M. Ras, J.-P. Steyer, O. Bernard, Temperature effect on microalgae: a crucial factor for outdoor production, Reviews in Environmental Science and Bio/Technology, 12 (2013) 153-164.
[30] H. Zhang, R. Zeng, D. Chen, J. Liu, A pivotal role of vacuolar H+-ATPase in regulation of lipid production in *Phaeodactylum tricornutum*, Scientific reports, 6 (2016) 1-17.
[31] B. Moss, The influence of environmental factors on the distribution of freshwater algae: an experimental study: II. The role of pH and the carbon dioxide-bicarbonate system, The Journal of Ecology, (1973) 157-177.
[32] Y. Azov, Effect of pH on inorganic carbon uptake in algal cultures, Applied environmental microbiology, 43 (1982) 1300-1306.
[33] M. Olaizola, Commercial development of microalgal biotechnology: from the test tube to the marketplace, Biomolecular engineering, 20 (2003) 459-466.
[34] J. Pandey, N. Pathak, A. Tiwari, Standardization of pH and light intensity for the biomass production of *Spirulina platensis*, Journal of Algal Biomass Utilization, 1 (2010) 93-102.
[35] K. Ying, W. Zimmerman, D. Gilmour, Effects of CO and pH on growth of the microalga *Dunaliella salina*,

Journal of Microbial and Biochemical Technology, 6 (2014) 167-173.
[36] Z. Amini Khoeyi, J. Seyfabadi, Z. Ramezanpour, Effect of light intensity and photoperiod on biomass and fatty acid composition of the microalgae, *Chlorella vulgaris*, Aquaculture International, 20 (2012) 41-49.
[37] J. Seyfabadi, Z. Ramezanpour, Z. Amini Khoeyi, Protein, fatty acid, and pigment content of *Chlorella vulgaris* under different light regimes, Journal of Applied Phycology, 23 (2011) 721-726.
[38] M.N. Metsoviti, G. Papapolymerou, I.T. Karapanagiotidis, N. Katsoulas, Effect of Light Intensity and Quality on Growth Rate and Composition of *Chlorella vulgaris*, Plants (Basel, Switzerland), 9 (2019).
[39] A. Amanullah, C.M. McFarlane, A.N. Emery, A.W. Nienow, Scale-down model to simulate spatial pH variations in large-scale bioreactors, Biotechnology and bioengineering, 73 (2001) 390-399.
[40] Z.I. Khalil, M.M. Asker, S. El-Sayed, I.A. Kobbia, Effect of pH on growth and biochemical responses of *Dunaliella bardawil* and *Chlorella ellipsoidea*, World journal of microbiology & biotechnology, 26 (2010) 1225-1231.
[41] B.S. Bamba, P. Lozano, F. Adjé, A. Ouattara, M.A. Vian, C. Tranchant, Y. Lozano, Effects of Temperature and Other Operational Parameters on *Chlorella vulgaris* Mass Cultivation in a Simple and Low-Cost Column Photobioreactor, Applied biochemistry and biotechnology, 177 (2015) 389-406.
[42] J. Masojídek, J. Kopecký, L. Giannelli, G. Torzillo, Productivity correlated to photobiochemical performance of *Chlorella* mass cultures grown outdoors in thin-layer cascades, Journal of Industrial Microbiology and Biotechnology, 38 (2011) 307-317.
[43] A. Kumar, S. Ergas, X. Yuan, A. Sahu, Q. Zhang, J. Dewulf, F.X. Malcata, H. van Langenhove, Enhanced $CO_{(2)}$ fixation and biofuel production via microalgae: recent developments and future directions, Trends in biotechnology, 28 (2010) 371-380.
[44] X. Hu, J. Zhou, G. Liu, B. Gui, Selection of microalgae for high CO_2 fixation efficiency and lipid accumulation from ten *Chlorella* strains using municipal wastewater, Journal of Environmental Sciences, 46 (2016) 83-91.
[45] B. Zhao, Y. Su, Process effect of microalgal-carbon dioxide fixation and biomass production: a review, Renewable Sustainable Energy Reviews, 31 (2014) 121-132.